Positron microbeam study on vacancy generation caused by stress corrosion crack propagation in austenitic stainless steels

2011 J. Phys.: Conf. Ser. 262 012067

(http://iopscience.iop.org/1742-6596/262/1/012067)

Journal of Physics: Conference Series **262** (2011) 012067 doi:10.1088/1742-6596/262/1/012067

Positron microbeam study on vacancy generation caused by stress corrosion crack propagation in austenitic stainless steels

A Yabuuchi, M Maekawa and A Kawasuso
ASRC, Japan Atomic Energy Agency, 1233, Watanuki, Takasaki, Gunma 370-1292, Japan
E-mail: yabuuchi.atsushi@jaea.go.jp

Abstract. A stress-corrosion-cracked Type 304 austenitic stainless steel was investigated by the Doppler broadening of annihilation radiation (DBAR) spectroscopy with a positron microbeam. Clear increase of S parameter was observed over 200-400 μm areas from the stress corrosion cracking (SCC) crack. From the comparison of the DBAR spectra obtained from the stress-corrosion-cracked sample and plastically deformed sample, the increase of S parameter around the SCC crack was attributed to plastic-deformation-induced vacancies.

1. Introduction

Stress corrosion cracking (SCC) is still a serious issue even in the low-carbon austenitic stainless steels which were developed as corrosion resistive materials for nuclear reactors. Recently, a hypothesis of the SCC crack propagation mediated by vacancies near the crack tip stress field is proposed [1-2]. Vacancies in austenitic stainless steels start to migrate at 250 °C [3-5] where a boiling-water reactor is operated. Thus, it is conceivable that vacancies play an important role in the high-temperature water SCC crack propagation mechanism. However, the origin of such vacancies has not yet been fully elucidated. In this study, to investigate the vacancy formation during the SCC crack propagation, an SCC-cracked Type 304 austenitic stainless steel was probed by a positron microbeam.

2. Experiment

All the samples used in this study were prepared from Type 304 austenitic stainless steel foils or plates that were sensitized at 650 °C for 24 hours in vacuum. The sensitized state is defined as a reference. These samples were subjected to the SCC test and plastic deformation test. In the SCC test, a sample ($5\times10\times0.03$ mm^3) having a notch was attached to a tensile holder with a tensile stress of approximately 100 MPa and exposed into boiling $MgCl_2$ water for an accelerated corrosion. The SCC crack started to appear after the corrosion treatment for 6 hours. In the plastic deformation test, a sample with a gauge width of 1 mm, a gauge length of 0.85 mm and a thickness of 50 μm was plastically deformed with a tensile stress up to the nominal strain of 20 %.

The above samples were transferred into a positron microbeam apparatus [6]. The SCC-cracked and deformed samples were scanned by a 20 keV positron microbeam with a diameter of approximately 10 μm with a scanning step of 100 μm and 40 μm, respectively, and DBAR measurements were carried out using a high-purity Ge detector. Accumulated total counts at each measurement were approximately 10^4. To monitor the presence of vacancy defects, the obtained DBAR spectra were characterized by S parameter, which is defined as the normalized peak intensity. All the S parameters were normalized to those obtained for the reference state. To identify the detected

defect species, the shapes of DBAR spectra were investigated in detail comparing with theoretical calculation.

3. Calculation of DBAR spectra

To interpret experimental DBAR data, theoretical calculations were carried out within the local density approximation [7]. The valence electron wavefunctions were calculated with the projector augmented-wave (PAW) method [8] using the ABINIT4.6.4 code [9]. The potentials and projectors were generated using the ATOMPAW code [10]. The valence electron configurations were $3s^2 3p^6 3d^6 4s^2$, $3s^2 3p^6 3d^5 4s^1$, $3s^2 3p^6 3d^8 4s^2$ for Fe, Cr and Ni atoms, respectively. A supercell including 23 Fe, 6 Cr and 3 Ni atoms with a 2×2×2 conventional fcc unit cell was constructed as an austenitic stainless steel. The cut-off energy of the plane wave basis set was 40 Ryd. The core electron wavefunctions were represented by the Slater function parameterized by Clementi and Roetti [11]. A self-consistent positron wavefunction was calculated based on the two-component density functional theory in order to minimize the energy functional [12]. The Borónski–Nieminen enhancement factor was adopted. The DBAR spectra were obtained by convoluting one-dimensional angular correlation of the annihilation radiation spectra obtained from the momentum density with the Gaussian resolution function having a half width of $3.92\times10^{-3}\ m_0c$.

4. Results and discussion

Figures 1(a) and 1(b) shows optical image and S parameter image, respectively, obtained from the SCC sample. It is seen that S parameter does not increased at the stress free region beside the initial notch. On the contrary, clear increase of S parameter is observed over 200-400 μm areas from the SCC crack. Figure 2(a) and 2(b) shows optical microscope image and S parameter image, respectively, obtained from the deformed sample. The increase of average S parameter in the gauge areas was 2.9 % after the deformation.

Figure 3 shows the experimental DBAR spectrum obtained from the deformed sample and the calculated DBAR spectrum for a monovacancy. To see the detailed spectrum shape, the original spectra were divided point-by-point by the experimental spectrum obtained from the undeformed sample and the calculated spectrum for the perfect lattice of a Type 304 austenitic stainless steel. The calculated spectrum is nicely reproduced the experimental one. Figure 4 shows the DBAR spectrum obtained from the gauge region of the deformed sample and near the crack region of the SCC sample. The original spectra were also divided by the reference spectrum. The DBAR spectrum of the SCC sample is in excellent agreement with that of the deformed sample.

The result shown in Fig. 1(b) suggests that lattice defects were formed near the crack due to the crack propagation. Plastic deformation is considered as an important factor giving rise to the change of S parameter near the crack due to the tensile stress concentrates on the crack tip. Thus, the DBAR spectrum of the deformed sample was measured in order to compare with that of the SCC sample. The spectrum shown in Fig. 3 indicates that the increase of S parameter brought by plastic deformation is caused by a formation of vacancy-type defects. The vacancy concentration introduced by plastic deformation may be given by

$$C_V = \eta \varepsilon^n \tag{1}$$

where η and n are constants and ε is the strain [13]. Assuming $\eta=10^{-2}$ and $n=2$, the vacancy concentration is approximately 4×10^{-4} at $\varepsilon=20$ %. Previous theoretical calculation studies have revealed that positrons are not localized strongly in the pure dislocation and the jog, in addition the positron lifetimes for the pure dislocation and the jog are close to the perfect-lattice value [14,15]. These perceptions imply that all implanted positrons are trapped at vacancy-type defects (e.g., vacancy-impurity complexes, small vacancy clusters or vacancies on the dislocation line). Similar DBAR spectra for the deformed sample and the SCC sample suggest that the plastic-deformation-induced vacancies are formed near the SCC crack. Such vacancies can migrate in the nuclear reactor operation temperature [3-5]. Therefore, it seems to be probable that vacancies migrate and accumulate

in grain boundaries of crack tips driven by a stress gradient. The corrosion is another important factor in the SCC. It is also possible that the vacancies observed near the crack were introduced by corrosion. Thus, the effect of corrosion on vacancy formation remains as a matter to be discussed further.

5. Conclusion

In this study, an SCC-cracked Type 304 austenitic stainless steel was probed by a positron microbeam. It was found that lattice defects were formed over 200-400 μm areas from the SCC crack. From the comparison of the DBAR spectra obtained from the SCC sample and the deformed sample, it is concluded that plastic-deformation-induced vacancies are introduced near the SCC crack during crack propagation. Further studies are needed to evaluate the effect of corrosion on vacancy formation in a Type 304 austenitic stainless steel.

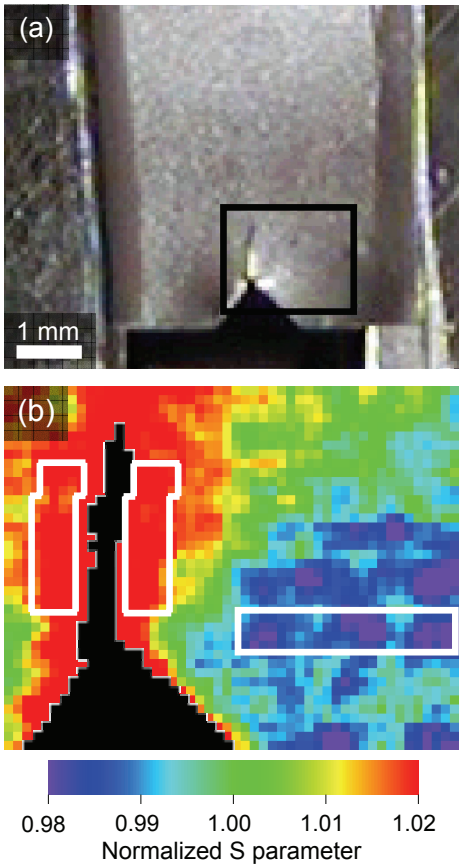

Figure 1. (a) Optical image of the SCC sample. The border in black indicates a scanned area (2.0×1.6 mm^2). (b) S parameter image of the SCC sample. The pixels in black correspond to the SCC crack gap or initial notch region. The borders in white indicate extraction area of the DBAR spectra as the reference and the region where S increased. Each pixel indicates 40×40 μm^2 region.

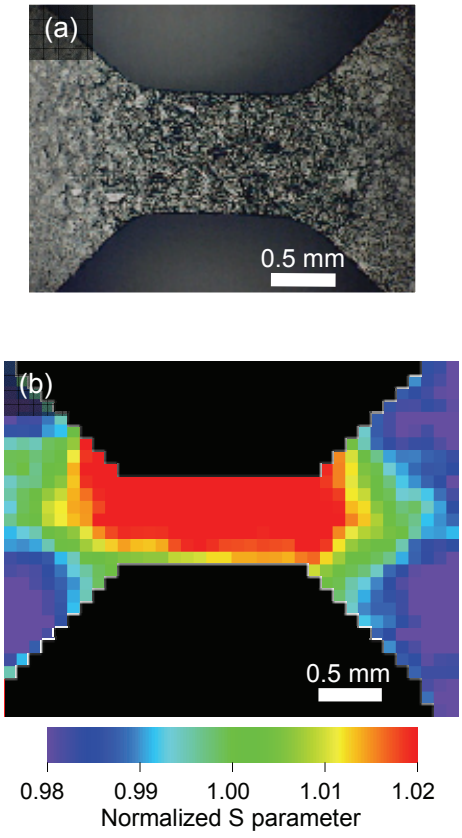

Figure 2. (a) Optical microscope image of the tensile test piece deformed by approximately 20 %. (b) S parameter image obtained from the tensile test piece after the deformation. Each pixel indicates 100×100 μm^2 region.

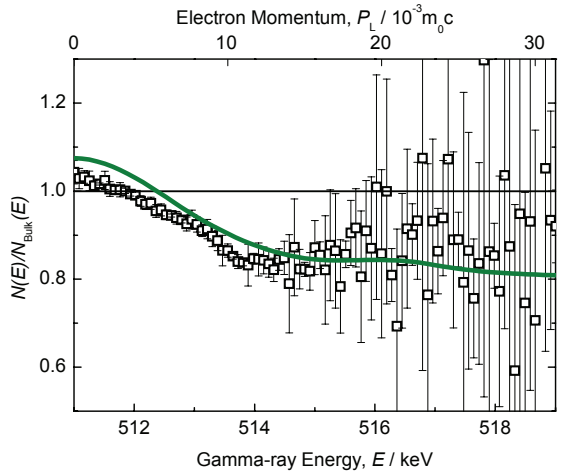

Figure 3. DBAR spectrum obtained from the gauge region of the deformed sample (open square). The original spectrum is divided by the spectrum of the undeformed sample. Solid line is the calculated DBAR spectra for a monovacancy in a Type 304 austenitic stainless steel.

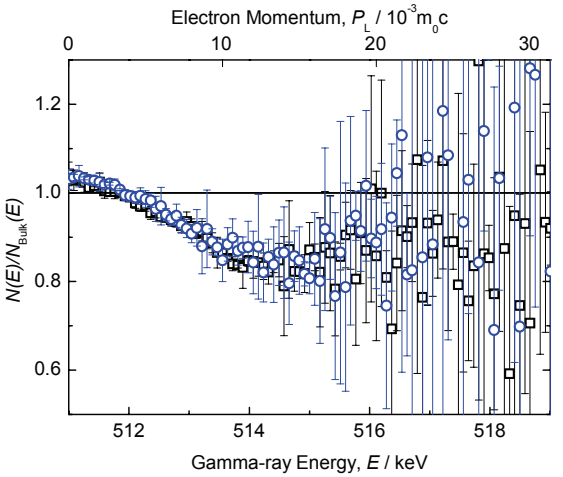

Figure 4. DBAR spectra obtained from the gauge region of the deformed sample (open square) and near the crack region of the SCC sample (open circle). Each original spectrum is divided by the spectrum obtained from the gauge region of the undeformed sample and the region where S unincreased in the SCC sample.

Acknowledgments

The present study was the result of "In-situ analysis of crack tips in stainless steels under tensile stress" entrusted to the Japan Atomic Energy Agency (JAEA) by the Ministry of Education, Culture, Sports, Science and Technology of Japan (MEXT) and was partially supported by the MEXT Grant-in-Aid for Young Scientists (B), No. 22760682, 2010.

References

[1] Staehle R W 2006 "*Proc. Int. Conf. Water Chem. Of Nucl. React. Sys.*," Jeju Is., Korea.
[2] Arioka K, Yamada T and Terachi T 2006 *INSS Journal* **13** 168-178 [in Japanese].
[3] Gil C L, de Lima A P, de Campos N A, Sperr P, Kögel G and Triftshäuser W 1990 *Radiat. Eff. Def. Solids* **112** 111-118.
[4] Dryzek J, Wesseling C, Dryzek E and Cleff B 1994 *Mater. Lett.* **21** 209-214.
[5] Arunkumar J, Abhaya S, Rajarman R, Amarendra G, Nair K G M, Sundar C S and Raj B 2009 *J. Nucl. Mater.* **384** 245-248.
[6] Maekawa M and Kawasuso A 2008 *Appl. Surf. Sci.* **255** 39-41.
[7] Puska M J and Nieminen R M 1994 *Rev. Mod. Phys.* **66** 841–897.
[8] Blöhl P E 1994 *Phys. Rev.* B **50** 17953-17979.
[9] Gonze X, Beuken J -M, Caracas R, Detraux F, Fuchs M, Rignanese G -M, Sindic L, Verstraete M, Zerah G, Jollet F, Torrent M, Roy A, Mikami M, Ghosez Ph, Raty J -Y, and Allan D C 2002 *Comput. Mater. Sci.* **25** 478–492.
[10] Holzwarth N A W, Tackett A R and Matthews G E 2001 *Comput. Phys. Commun.* **135** 329–347.
[11] Clementi E and Roetti C 1974 *At. Data Nucl. Data Tables* **14** 177-478.
[12] Borónski E and Nieminen R M 1986 *Phys. Rev.* B **34** 3820–3831.
[13] Russell B 1963 Phil. Mag. **88** 615-630.
[14] Kamimura Y, Tsutsumi T and Kuramoto E 1995 *Phys. Rev.* B **52** 879-885.
[15] Kamimura Y, Tsutsumi T and Kuramoto E 1997 *J. Phys. Soc. Jpn.* **66** 3090-3096.